

Representation of non-rectangular boundaries in numerical simulations of natural convection flows in reservoir sidearms

Dittko, K.A.¹, M.P. Kirkpatrick¹ and S.W. Armfield¹

¹ *School of Aerospace, Mechanical, Mechatronic Engineering, University of Sydney.*
Email: k.dittko@aeromech.usyd.edu.au

Abstract: This research investigates turbulent natural convection in a triangular cavity heated by solar radiation. This is a simplified model representing the sidearm of a lake or water reservoir. Lateral temperature gradients exist due to the varying depth of the cavity, resulting in lateral circulation. These flows are important in a reservoir as they can carry with them particles and various pollutants, transporting and mixing them with the central section. Therefore study in this area is important in water quality management.

The solar radiation model consists of a heat flux from the sloped bottom boundary as well as an internal heating source term in the body of the water. The heat flux at the bottom boundary induces natural convection including convective plumes and a large scale circulation, while the internal heating acts to stabilise the flow through the generation of a stable density stratification. Numerical simulations up to a Rayleigh number of 10^9 have been run to investigate different approaches for representing the oblique boundary on a Cartesian grid using the finite volume method.

In the initial case a Cartesian grid with a stepped boundary for the sloping bottom was used. This approach gave relatively poor results. The steps appear to provide local perturbations in the velocity field that can trigger thermal plumes. The thermal plumes are seen rising from the sloped boundary at intervals proportional to the step size, and the number and location of plumes was found to vary significantly as the grid resolution was changed. Refining the grid to a sufficient degree near the boundary is not practical for anything other than a basic 2D model, since this requires that the simple Cartesian grid be fine over the entire domain.

Two alternative approaches are investigated; using a grid with cell aspect ratio equal to the slope of the bottom boundary, and sloping the grid so that it is aligned with the boundary. Representing the bottom boundary using an Immersed Boundary method is also currently being implemented. The Immersed Boundary method involves using forcing terms in the flow equations to represent an interface or the surface of an object. The surface may split a computational cell so that the grid does not need to be aligned with the surface.

Other approaches commonly used include cut cells for Cartesian grids, or body fitted coordinates with an unstructured mesh. The methods investigated here have the advantage of greatly simplifying grid generation and boundary condition implementation, while still being less computationally expensive than the alternatives.

The methods investigated aim to remove the local fluctuations that induce the early appearance of thermal plumes. Changing the aspect ratio of the cells allows the Cartesian grid to remain aligned with the vertical direction, however it is not possible to refine the grid close to the boundary. Aligning the grid with the sloped bottom surface enables the grid to be refined close to this boundary, however the vertical plumes and density stratification are now skewed with respect to the grid. This increases the magnitude of the numerical errors associated with flux terms in the internal regions of the flow.

Keywords: *Immersed Boundary Method (IBM), Natural Convection, Complex Geometry*

1 INTRODUCTION

The flow domain investigated here is a 2 dimensional triangle as shown in Figure 1. Triangle cavities of this type have relatively little coverage in the literature. One good example however is work by Lei & Patterson (2002), which will be used to verify these simulations. The work of Lei & Patterson (2002) uses a curvilinear grid to ensure the sloped bottom is aligned with the grid. This is convenient for representing the boundary although it involves more complex formulation of equations and will also be less applicable to any future work that may involve more complex geometry. In contrast the work in this paper uses a number of different implementations of a Cartesian grid.

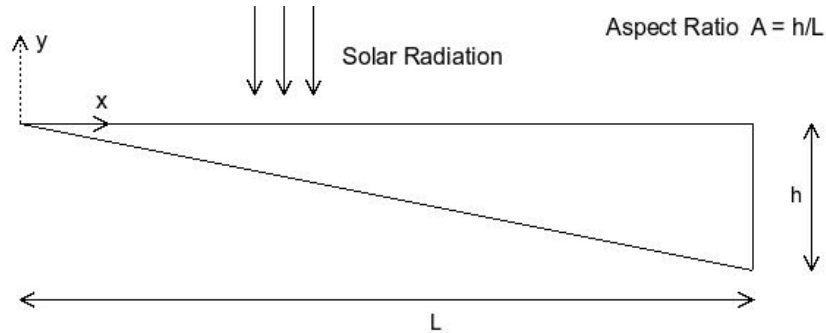


Figure 1. Flow domain.

The important parameters describing this problem are the Rayleigh number, Prandtl number, and aspect ratio of the cavity. In order to remain consistent with Lei & Patterson (2002), an aspect ratio of 0.1 has been maintained throughout this paper.

An important feature of the triangle cavity problem is that the heating is modelled as a solar flux through the top surface. This provides an internal heating source that decreases with depth as the radiation is gradually absorbed as it penetrates the water. This process may be modelled using Beer's Law (see for example Rabl & Nielsen (1975)). Lei & Patterson (2002) approximate the attenuation coefficient as having a single value across all wavelengths, so the source term for internal heating in the cavity becomes (see also Farrow & Patterson (1994))

$$S = H_0 \eta e^{\eta y},$$

where H_0 is the surface heating intensity, y the negative distance through which the radiation has travelled, and η the attenuation coefficient.

This relation shows that the heating intensity is greatest close to the surface and decreases with depth. Also since it is not horizontally dependent, this input does not induce circulation in the cavity, but in fact stabilises the cavity since warmer water is on top of colder water.

In shallow areas a significant portion of the radiation penetrates the entire depth of the water, heating the bottom surface and consequently heating the bottom fluid layer when this heat is transferred to the water. It is for this reason that the shallow section of a reservoir is interesting. Heating at the bottom boundary does induce instability in the flow, and is also horizontally variable since the depth varies across the cavity. Following Lei & Patterson (2002) this is modelled as a boundary flux,

$$\frac{\partial T}{\partial \hat{n}} = -\frac{1}{k} H_0 e^{-A\eta x},$$

where T is the temperature, \hat{n} the direction normal to the boundary, k the thermal diffusivity and A the aspect

ratio of the cavity so that $y = -Ax$ at the boundary. This assumes that all heat reaching the surface is absorbed and then immediately transferred to the fluid by convection.

The flow in the cavity is dependent on the Rayleigh number, defined as

$$Ra = GrPr,$$

where Pr is the Prandtl number and Gr the Grasshof number

$$Gr = \frac{g\beta H_0 h^4}{\nu^2 k},$$

where g is the acceleration due to gravity, β the coefficient of thermal expansion and ν the kinematic viscosity. The Grasshof number in this problem is defined using H_0 since the height of the cavity changes across the width, as does the temperature difference between the top and bottom fluid layers.

2 METHOD

All simulations are performed using the PUFFIN code (Kirkpatrick (2002) and Kirkpatrick et al. (2003)) which solves the Boussinesq form of the unsteady Navier-Stokes equations on a Cartesian grid. The code has been used to simulate flows ranging from industrial flows such as swirling jets (Ranga Dinesh & Kirkpatrick (2009)) to environmental flows including purging of saltwater in a cavity by an overflow of freshwater (Kirkpatrick & Armfield (2005)) and atmospheric boundary layer flow over a mountain (Kirkpatrick & Armfield (2009)).

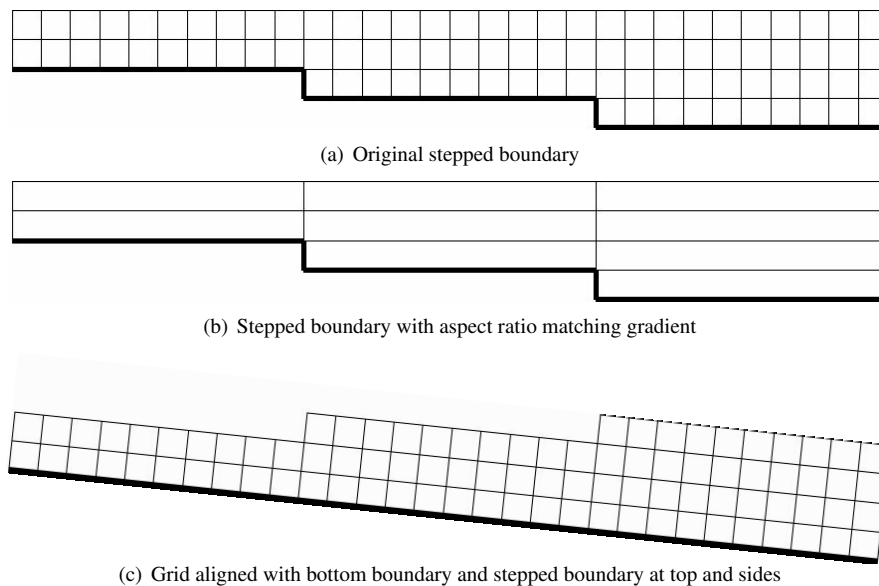


Figure 2. Different methods of setting up a Cartesian grid: (a) is a standard non-stretched grid resulting in a stepped bottom boundary, (b) has stretched cells such that the aspect ratio matches that of the boundary gradient, and (c) has the entire grid tilted such that it is aligned with the bottom boundary, and the top and side boundaries are now stepped.

Four main alternatives for grid setup are investigated here. These are a standard step cell bottom boundary (Figure 2(a)), a stepped boundary on a grid in which the cell aspect ratio exactly matches the boundary gradient (Figure 2(b)), a sloped grid such that the grid is aligned with the bottom boundary with stepped boundaries on the top and side (Figure 2(c)), and finally the immersed boundary method on the bottom surface (Figure 3).

2.1 Immersed Boundary Method

The Immersed Boundary Method (IBM) used is based primarily on work presented by Gao et al. (2007). The method uses a second order Taylor series expansion to approximate the velocity at ghost cells located immediately outside the boundary. In this 2D case with a straight boundary the approximation is made using the cells as shown in Figure 4. The aim is to set values at the ghost cells that give the desired conditions at the actual boundary location, even though the actual boundary location usually does not coincide with a grid node.

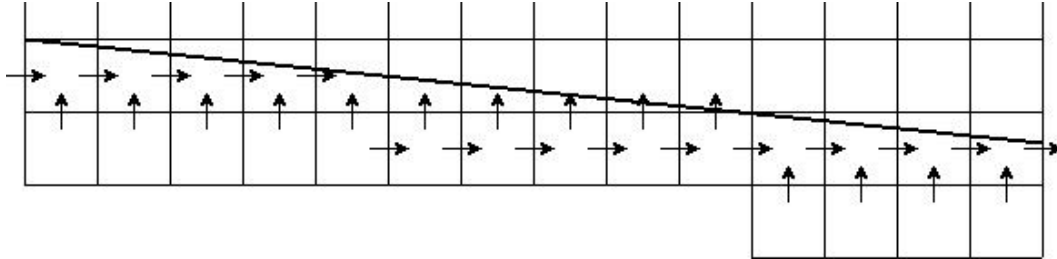


Figure 3. Immersed boundary. Velocity vectors shown are ghost values.

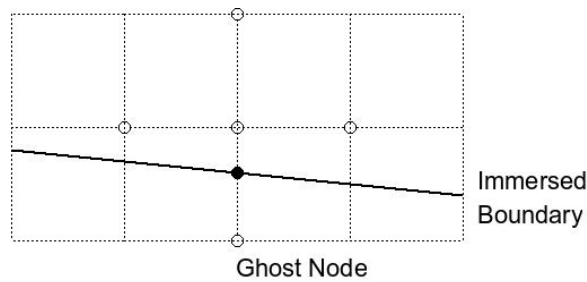


Figure 4. The value at the ghost node is calculated using the four points inside the flow shown. The ghost node will cause the value at the boundary itself to be set to a desired value, even though it does not fall on a node.

Like Gao et al. (2007) the PUFFIN code uses a finite volume, fractional step method with a staggered grid. This results in the nodes for W velocity being offset to the nodes for the U velocity (Figure 3).

Once the desired ghost node values are calculated as described above, they are implemented in the code using a forcing function \mathbf{f} , that is added to the momentum equation

$$\frac{\partial \mathbf{u}}{\partial t} + \mathbf{u} \cdot \nabla \mathbf{u} = -\frac{1}{\rho} \nabla p + \nu \nabla^2 \mathbf{u} + \mathbf{f}.$$

The semi-discrete form of the momentum equation is then represented by (see Fadlun et al. (2000))

$$\frac{u^{n+1} - u^n}{\delta t} = RHS^{n+\frac{1}{2}} + f^{n+\frac{1}{2}},$$

which by setting our desired condition $u^{n+1/2} = V^{n+1/2}$ then gives

$$f^{n+\frac{1}{2}} = -RHS^{n+\frac{1}{2}} + \frac{V^{n+1} - u^n}{\delta t}.$$

Here RHS comprises the convective, viscous and pressure gradient terms and V is the desired velocity at the boundary.

Implementation of the IBM is still underway so results will not be presented in this paper.

3 RESULTS

Figure 5 shows two simulations with identical conditions, with only the grid size changed. Changing the grid size has the effect of automatically changing the step size as well. It is clear that the occurrence of the thermal plumes is being affected by this change in step size. In fact there is almost exactly one thermal plume rising from each step in both the fine and coarse grid case, resulting in double the number of thermal plumes in the fine grid case since the steps are half the size. Tests were performed on grids of resolution up to 1000×100 with no sign of convergence of the solution with increasing resolution. This indicates singular behaviour at the boundary. A likely cause of this behaviour is the artificial perturbations introduced into the velocity field by the step changes in the boundary.

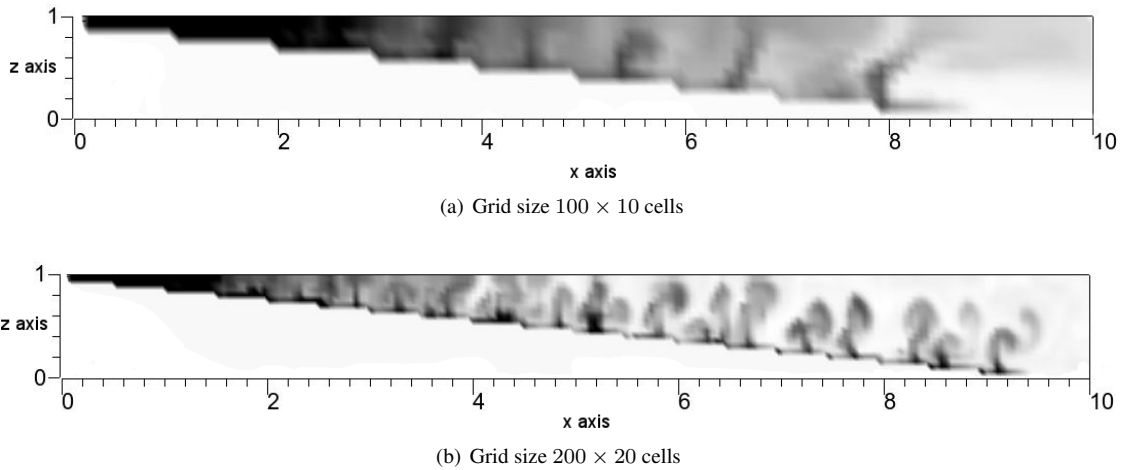


Figure 5. Temperature colour plot at $t = 120s$ for stepped grid with $Ra = 1 \times 10^9$, $Pr = 7.0$, cell aspect ratio 1 (10 cells per step). Temperature range is $0.3K$. (a) coarse grid, (b) fine grid.

In contrast Figure 6 shows the same setup conditions again, however this time with a grid formed such that the cell aspect ratio matches the boundary gradient. The number of thermal plumes is very similar in each case, indicating that the number of thermal plumes is no longer influenced by the step size. This is expected since by having cell aspect ratio equal to the boundary gradient, the continuity equation will force the first layer of velocity vectors to be tangential to the boundary, hence there will be no artificial perturbations. However it is also noted that the plumes have a very different appearance with this grid when compared to the case with a cell aspect ratio of 1. The plumes appear to keep a much more structured, symmetrical shape, rising vertically with much less spreading. In the square grid case they spread more rapidly and in a far less organised manner. This is most likely due to the difference in vertical grid resolution.

Results for the sloped grid are shown in Figure 7. They demonstrate that removing the discrete steps from the bottom boundary leads to a significant improvement, with little change in number of thermal plumes between the grid sizes. Even though there is now a stepped boundary on the top and side, this appears to have little effect on the flow characteristics. This is in agreement with Lei & Patterson (2002) who found that the top boundary had little effect on the flow. They found that representing the top with either a Dirichlet or zero flux boundary in fact had a negligible effect.

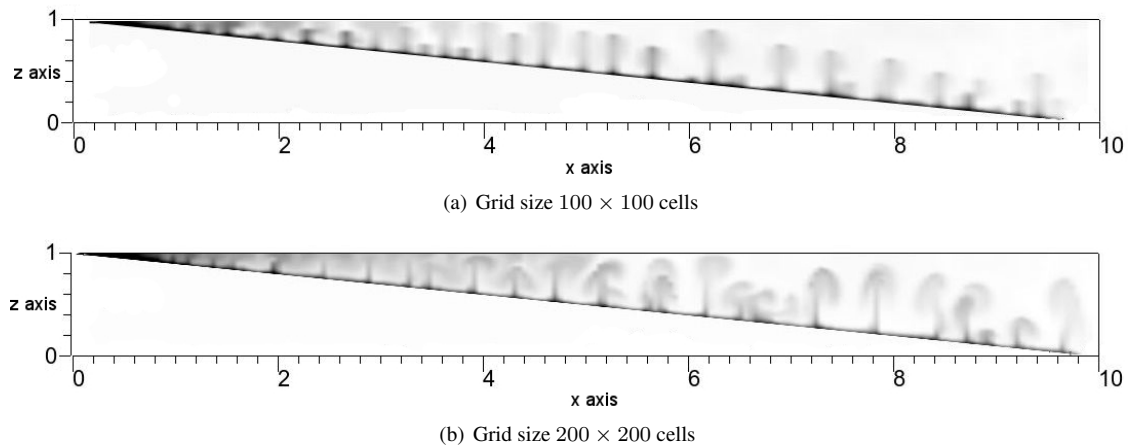


Figure 6. Temperature colour plot at $t = 120s$ for stepped grid with $Ra = 1 \times 10^9$, $Pr = 7.0$, cell aspect ratio 0.1 (1 cell per step). Temperature range is $0.2K$. (a) course grid, (b) fine grid.

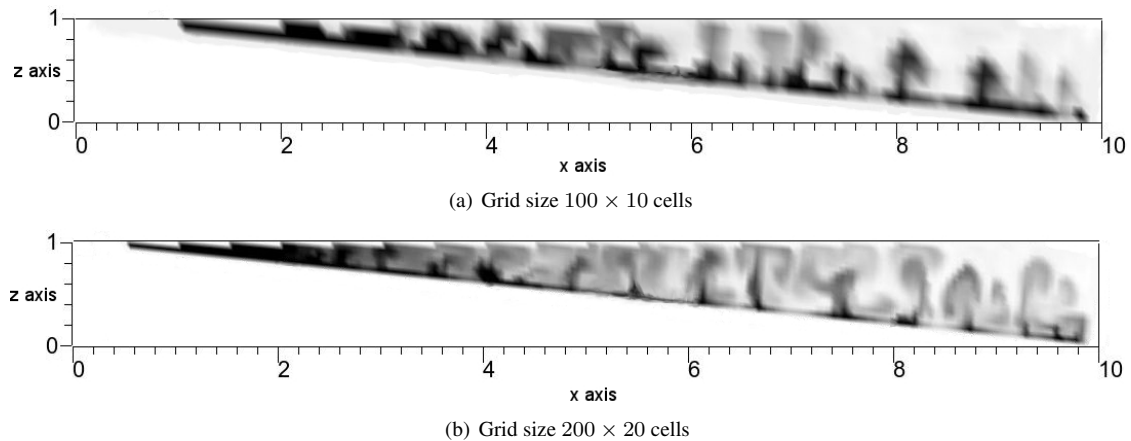


Figure 7. Temperature colour plot at $t = 120s$ for grid sloped in line with bottom boundary and $Ra = 1 \times 10^9$, $Pr = 7.0$. Temperature range is $0.3K$. (a) course grid, (b) fine grid.

4 CONCLUSIONS

The numerical simulations shown here have demonstrated that in the problem of a triangle cavity heated by solar radiation the method of representing the bottom boundary has a large effect on the accurate representation of the Rayleigh-Benard instability. In particular we see that the flow changes significantly as we change the grid size when a stepped boundary is used.

Changing the aspect ratio of the cells to be equal to the slope of the boundary greatly improved the results, however this is far from flexible if a simulation was considered with slightly more complex geometry. It is also more computationally expensive since for small gradients, in order to get sufficient horizontal resolution, vertical resolution must be far greater than would otherwise be required.

Sloping the grid to align with the bottom boundary also greatly improved the results. This method however is also not flexible enough for complex geometry cases, and in addition has the effect of the density stratification and thermal plumes no longer being aligned with the grid, meaning the magnitude of numerical errors is likely to increase.

The Immersed Boundary Method is currently being implemented. This will allow removal of the stepped boundary without requiring the grid to be sloped, or the use of cells of a particular aspect ratio. The local fluctuations caused by the boundary representations already modelled will be removed, so it is expected that the results will show far more accurate representation of the Rayleigh-Benard instability.

Once the computer model being developed here is complete it will be used to perform a series of high resolution simulations of reservoir sidearms. We intend to use these results as a basis for a scaling analysis of the flow. We hope that this analysis will yield simple parameterizations for the transport processes, which would then be useful for representing sidearm transport in larger scale lake models.

References

- Fadlun, E. A., Verzicco, R., Orlandi, P. & Mohd-Yusof, J. (2000), 'Combined immersed-boundary finite-difference methods for three-dimensional complex flow simulations', *Journal of Computational Physics* 161(1), 35–60.
- Farrow, D. E. & Patterson, J. C. (1994), 'The daytime circulation and temperature structure in a reservoir sidearm', *International Journal of Heat and Mass Transfer* 37(13), 1957–1968.
- Gao, T., Tseng, Y. H. & Lu, X. Y. (2007), 'An improved hybrid cartesian/immersed boundary method for fluid-solid flows', *International Journal for Numerical Methods in Fluids* 55(12), 1189–1211.
- Kirkpatrick, M. P. (2002), A large eddy simulation code for industrial and environmental flows, PhD thesis, The University of Sydney.
- Kirkpatrick, M. P. & Armfield, S. W. (2005), 'Experimental and large eddy simulation results for the purging of salt water from a cavity by an overflow of fresh water', 48, 341–359.
- Kirkpatrick, M. P. & Armfield, S. W. (2009), 'Open boundary conditions in numerical simulations of incompressible unsteady flow', *ANZIAM J* 50, C760–C773.
- Kirkpatrick, M. P., Armfield, S. W. & Kent, J. H. (2003), 'A representation of curved boundaries for the solution of the Navier-Stokes equations on a staggered three-dimensional Cartesian grid', 184, 1–36.
- Lei, C. W. & Patterson, J. C. (2002), 'Unsteady natural convection in a triangular enclosure induced by absorption of radiation', *Journal of Fluid Mechanics* 460, 181–209.
- Rabl, A. & Nielsen, C. E. (1975), 'Solar ponds for space heating', *Solar Energy* 17(1), 1–12.
- Ranga Dinesh, K. & Kirkpatrick, M. P. (2009), 'Study of jet precession, recirculation and vortex breakdown in turbulent swirling jets using les', *Computers and Fluids* 38(6), 1232–1242.